

# Hyperfine Interaction-Driven Suppression of Quantum Tunneling at Zero Field in a Ho(III) Single-Ion Magnet

Yan-Cong Chen,<sup>[a]</sup> Jun-Liang Liu,\*<sup>[a]</sup> Wolfgang Wernsdorfer,<sup>[b][c][d]</sup> Dan Liu,<sup>[e]</sup> Liviu F. Chibotaru,<sup>[e]</sup> Xiao-Ming Chen,<sup>[a]</sup> and Ming-Liang Tong\*<sup>[a]</sup>

**Abstract:** An extremely rare non-Kramers holmium(III) single-ion magnet (SIM) is reported to be stabilized in the pentagonal-bipyramidal geometry based on phosphine oxide with a high energy barrier of 237(4) cm<sup>-1</sup>. The suppression of quantum tunneling of magnetization (QTM) at zero field and the hyperfine structures originating in field-induced QTMs can be observed even from the field-dependent alternate-current (AC) magnetic susceptibility in addition to single-crystal hysteresis loops. This dramatic dynamic is attributed to the combination of the favorable crystal-field environment and the hyperfine interactions arising from <sup>165</sup>Ho (*I* = 7/2) with a natural abundance of 100 %.

Molecular magnetism has attracted broad interest among chemists, physicists and materials scientists as a highly multidisciplinary research area requiring combined effort. Since the discovery of {Mn<sub>12</sub>ac}, single-molecule magnets (SMMs) have shown increasing competitiveness as promising candidates for high-density information storage, quantum processing and spintronics.<sup>1,2</sup> In recent years, lanthanide SMMs opened a new avenue due to their generally high magnetic anisotropy, which can achieve high energy barriers.<sup>3</sup> The most common SMMs are based on Dy(III)<sup>4</sup> and Er(III),<sup>5</sup> both of which are Kramers ions with half-integer spins. For non-Kramers ions, however, only Tb(III) SMMs have been extensively studied since the report of the famous [(Pc)<sub>2</sub>Tb]<sup>+</sup> double decker.<sup>6</sup> The cases for its neighbor, Ho(III), are extremely rare with only [(Pc)<sub>2</sub>Ho]<sup>+</sup>, [HoP<sub>5</sub>W<sub>30</sub>O<sub>110</sub>]<sup>12-</sup>, [Ho(W<sub>5</sub>O<sub>18</sub>)<sub>2</sub>]<sup>19-</sup>, HoSc<sub>2</sub>N@C<sub>80</sub> and [Ho<sub>5</sub>O(OPr)<sub>13</sub>].<sup>7</sup> Without the Kramers theorem, which prevents the double degeneracy of the electronic ground microstates from splitting under zero magnetic field, the fast quantum tunneling of magnetization for non-Kramers ions is easily introduced by a

transverse crystal field. In this respect, the vast majority of complexes without specific coordination symmetries are less likely to bear the observable slow relaxation of magnetization.

The pentagonal-bipyramidal geometry, toward *D*<sub>5h</sub> symmetry, has been shown to favor high-performance SMMs, as the mixing of the magnetic states from crystal-field terms can be greatly reduced. This situation is highly important for the monometallic SMMs called single-ion magnets, since their QTM cannot be suppressed by intramolecular magnetic interactions as in the multimetallic SMMs. Through rational design and experimental optimization, extremely high energy barriers and high blocking temperatures can be achieved inspired by this idea.<sup>4d-4h</sup> Moreover, only when the crystal-field contribution is minimized can we investigate certain subtle factors of QTM, such as hyperfine interaction.<sup>7a,8</sup>

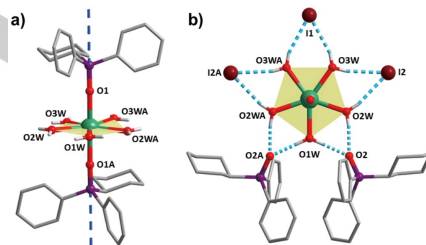


**Figure 1.** a) Coordination environment of Ho(III) in **1**. The blue dashed line represents the orientation of the main magnetic axes of the lowest Kramers doublets. b) Outer coordination sphere connected by hydrogen bonds in **1**. H atoms of CyPh<sub>2</sub>PO are omitted for clarity. Color codes: Ho, green; P, purple; I, brown; O, red; C, gray; H, light gray. Symmetry code (A): 1-x, y, 0.5-z.

Here, we report a pentagonal-bipyramidal Ho(III) model complex, [Ho(CyPh<sub>2</sub>PO)<sub>2</sub>(H<sub>2</sub>O)<sub>5</sub>]<sub>3</sub>·2(CyPh<sub>2</sub>PO)·H<sub>2</sub>O·EtOH (**1**), based on phosphine oxide and characterized as an extremely rare Ho-SIM. Multiple peaks on the field dependence of the relaxation time determined by AC susceptibility and the steps on the ultra-low temperature magnetic hysteresis loops are assigned to the hyperfine interactions between the *J* = 8 electronic spin and *I* = 7/2 nuclear spin of <sup>165</sup>Ho. In combination with the *ab initio* calculations, these findings show that the compressed pentagonal-bipyramidal geometry in **1** results in a high energy barrier, and surprisingly, the QTM at zero field is suppressed rather than sped up by the hyperfine interactions, whereas field-induced QTMs are enabled at specific positions with avoided level crossing. We have demonstrated that non-Kramers holmium(III) can also be effectively utilized for the rational design of high-performance SMMs when the interplay between magnetic anisotropy and hyperfine interactions is nicely tailored.

[a] Y.-C. Chen, Dr. J.-L., Liu, Prof. Dr. X.-M. Chen, Prof. Dr. M.-L. Tong  
Key Laboratory of Bioinorganic and Synthetic Chemistry of Ministry  
of Education, School of Chemistry, Sun Yat-Sen University,  
Guangzhou 510275, P. R. China  
E-mail: liujiang5@mail.sysu.edu.cn, tongml@mail.sysu.edu.cn

[b] Prof. Dr. W. Wernsdorfer  
Institut Néel, CNRS & Université Joseph Fourier, BP 166, 25  
avenue des Martyrs, 38042 Grenoble Cedex 9, France

[c] Prof. Dr. W. Wernsdorfer  
Institute of Nanotechnology, Karlsruhe Institute of Technology,  
76344 Eggenstein-Leopoldshafen, Germany

[d] Prof. Dr. W. Wernsdorfer  
Physikalisches Institut, Karlsruhe Institute of Technology, 76131  
Karlsruhe, Germany

[e] D. Liu, Prof. Dr. L. F. Chibotaru  
Theory of Nanomaterials Group and INPAC—Institute of Nanoscale  
Physics and Chemistry, Katholieke Universiteit Leuven,  
Celestijnenlaan 200F, 3001 Leuven, Belgium

The molecular structure of **1** is similar to its Dy(III) derivatives,<sup>4e</sup> with two strong CyPh<sub>2</sub>PO ligands in the axial positions and five coordinated waters in the equatorial plane (Figure 1). A crystallographic  $C_2$  axis passes through Dy1-O1W and provides an additional two-fold symmetry. The local environment of the Ho(III) ion can be regarded as a compressed pentagonal bipyramid with axial Ho–O bond lengths of 2.198 Å and an average equatorial Ho–O bond length of 2.364 Å. The O1–Ho–O1A angle is almost linear, up to 177.9(4) $^\circ$ , and the Continuous Shape Measures (CShM) calculation value deviated from ideal  $D_{5h}$  by as little as 0.160. Furthermore, this core is stabilized by a five-pointed star established by hydrogen bonds among the five coordinated waters, the second coordinate sphere of two CyPh<sub>2</sub>PO ligands, and three I<sup>–</sup> ions. The discrete molecules pack in an orthorhombic C222<sub>1</sub> space group with the nearest Ho...Ho distance of 14.08 Å, and the main anisotropic axis (O1–Ho–O1A) lies 31° from the c axis (Figure S1).

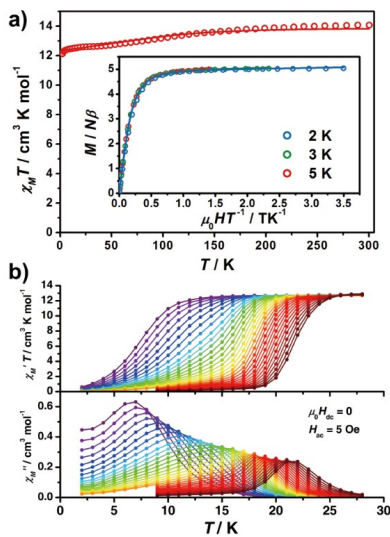


**Figure 2.** **a)** Temperature dependence of the molar magnetic susceptibility  $\chi_M T$  products for **1** under a 0.1 T DC field. Inset: magnetization ( $M$ ) versus  $H/T$  for **1**. The solid lines correspond to the *ab initio* calculations. **b)** Temperature dependence of the in-phase  $\chi_M T$  product and out-of-phase  $\chi_M''$  for **1** in a zero DC field with an AC frequency of 1–1488 Hz.

The variable-temperature magnetic susceptibilities measured on polycrystalline samples of **1** under a 0.1 T DC field (Figure 2a) show a stepwise decrease upon cooling from 14.1  $\text{cm}^3 \text{K mol}^{-1}$  at 300 K to 12.1  $\text{cm}^3 \text{K mol}^{-1}$  at 2 K with a plateau near 30 K, which indicates the presence of excited states located near the measuring window. Additionally, the nicely overlapping  $M$  vs.  $H/T$  curves at low temperatures (Inset of Figure 2a) provide evidence of the far-separated excited energy levels. The temperature dependence of the AC magnetic susceptibilities in a zero DC field (Figure 2b) shows nice peaks below 22 K, which is extremely rare for Ho(III). As a non-Kramers ion, Ho(III) usually has quite fast QTM, and thus slow relaxation is very difficult to observe. In this case, the highly compressed local environment combined with the pseudo five-

fold symmetry (pseudo  $D_{5h}$ ) greatly reduces the mixing of  $|m_J\rangle$  states from crystal-field terms, making **1** a rare Ho(III) SIM even at zero field.

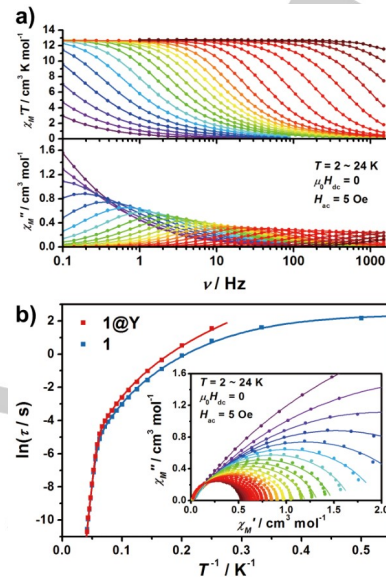


**Figure 3.** **a)** Frequency dependence of the in-phase  $\chi_M'$  and out-of-phase  $\chi_M''$  in a zero DC field for **1**. **b)** Temperature dependence of the relaxation time  $\tau$  in a zero DC field for **1** (red) and **1@Y** (blue). The solid line is the best fit to the multiple relaxation equation. Inset: Cole-Cole plot for AC susceptibilities under a zero DC field for **1**.

A detailed measurement of the frequency dependence of the AC magnetic susceptibilities in a zero DC field (Figure 3a) clearly shows the competition of multiple relaxation processes of **1**. The relaxation times are extracted by a generalized Debye model. Then, the temperature dependence of the relaxation time can be fitted with the equation  $\tau^1 = \tau_0^{-1} \exp(-U_{\text{eff}}/k_B T) + CT^n + \tau_{\text{QTM}}^{-1}$ . At high temperatures, the relaxation times perfectly obey the Arrhenius law corresponding to the Orbach process with  $U_{\text{eff}} = 237(4)$   $\text{cm}^{-1}$ ,  $\tau_0 = 1.7 \times 10^{-11}$  s. At low temperatures, the relaxation is generally dictated by the Raman process with  $n = 4.22(4)$  and finally limited by  $\tau_{\text{QTM}} = 11.6(8)$  s (Figure 3b). The diluted sample, **1@Y**, shows similar behavior with  $U_{\text{eff}} = 245(4)$   $\text{cm}^{-1}$ ,  $\tau_0 = 9.9 \times 10^{-12}$  s and  $n = 4.40(4)$  but without a limiting  $\tau_{\text{QTM}}$  within the measuring window, indicating that the QTM in **1** arising from the intermolecular magnetic interactions can somehow be greatly weakened through dilution. The *ab initio* calculations (see SI)<sup>9</sup> based on the crystal structure show that the first and second excited doublets are located at 199  $\text{cm}^{-1}$  and 227  $\text{cm}^{-1}$ , respectively (Figures S5 and S11). Given the much larger transition magnetic moment to the second excited doublet compared to the first (Figure S11) and the relatively small difference in their energies, the Orbach relaxation will proceed via the second excited doublet, as in other Ln complexes with high axiality.<sup>10</sup>

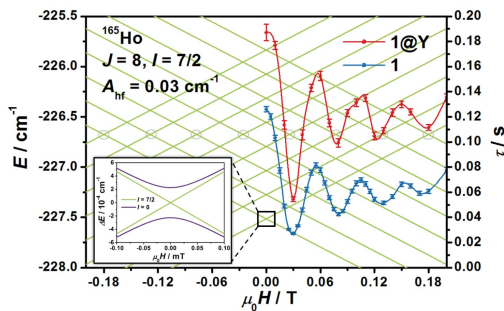


**Figure 4.** Field dependence of the relaxation time (right axis) measured by AC susceptibility at 8 K for **1** (blue) and **1@Y** (red), compared with the longitudinal Zeeman energy diagram (green, left axis) for the ground hyperfine states calculated with the hyperfine-interaction parameter of  $A_{\text{hf}} = 0.03 \text{ cm}^{-1}$  and the crystal-field parameters ( $k = 2, 4, 6; q = -k$  to  $+k$ ) from *ab initio* calculations (Table S7). The positions with avoided level crossings are marked with gray circles. Inset: Zoom view around zero field for the lowest doublet showing the difference with (green) and without (purple) hyperfine interactions.

Interestingly, when a DC field is applied, the relaxation time for **1** obtained from AC susceptibility shows an unusual field dependence behavior compared with most of the reported SIMs to date: 1) the relaxation time for **1** is quite long at zero field, in contrast to the relaxation times under applied fields; 2) hyperfine-structure steps were observed, showing four negative peaks centered at approximately 0.03, 0.08, 0.13, and 0.18 T (Figure 4). In contrast to the normal single peak corresponding to the suppression of QTM and the presence of the direct process, the “abnormal” stepwise field-dependent dynamics for **1** suggests that the QTM is somewhat blocked at zero field, while applying an external DC field leads to faster quantum tunneling at certain specific points. A parallel experiment on the diluted sample **1@Y** shows that relaxation times only increase slightly without changing the peak positions. To some extent, it is confirmed that this behavior must come not from the intermolecular interactions but instead from the behavior of discrete molecules. Note that even with random orientations for the microcrystalline sample, the resonances of the hyperfine structures can be preserved instead of being smeared out.<sup>11</sup>

As the natural abundance for holmium is 100 %  $^{165}\text{Ho}$  with  $I = 7/2$ , the energy states of its electronic spin are in fact coupled with nuclear spin through hyperfine interactions. For **1**, the *ab initio* calculations show that the quasi-degenerate doublet from the  $^5\text{S}$  electronic configuration consist mostly (> 99.9 %) of  $m_J = \pm 8$ , which splits into  $2 \times (2I+1) = 16$  hyperfine states when coupled with  $I = 7/2$  (Table S8). Given the hyperfine-interaction parameter  $A_{\text{hf}} = 0.03 \text{ cm}^{-1}$  ( $\hat{H}_{\text{hf}} = A_{\text{hf}} J \hat{J}$ ) and the crystal-field parameters from the *ab initio* calculations ( $\hat{H}_{\text{cf}} = \sum B_k q \hat{O}_k q$ ;  $k = 2, 4, 6; q = -k$  to  $+k$ ; where  $\hat{O}_k q$  is the extended Stevens operator) (Table S7), the longitudinal Zeeman energy diagram can be nicely reproduced (Figure 4). A careful check reveals that only four positions (when  $H \geq 0$ , gray circles in Figure 4, with zoom view in Figure S7) can exhibit noticeable avoided level crossings within the calculation accuracy range. As the avoided level crossings correspond to the mixing of the states, the QTM is significant at these fields, which is consistent with the negative peaks of the relaxation times.

This behavior is partly similar to the case of  $[(\text{Pc})_2\text{Ho}]$ ,<sup>7a</sup> while the most obvious difference for **1** is the absence of observable QTM coming from the transverse magnetic field. Indeed, the mixing of the states from the crystal field has been greatly reduced by the axially compressed local environment, which stabilizes the largest  $m_J = \pm 8$  as the main components of the ground quasi-degenerate doublet, and the pseudo five-fold symmetry ( $D_{5h}$ ) minimizing the transverse anisotropy as well.

It should be particularly noted that the avoided level crossings near zero field cannot be observed when the nuclear spin is present here in **1** (inset of Figure 4), which means the hyperfine interaction here is playing the key role in suppressing the QTM at zero field. From a theoretical perspective, the integer electronic spin  $J = 8$ , coupled with the half-integer nuclear spin  $I = 7/2$  for  $^{165}\text{Ho}$ , shall be integrated into a Kramers system and gain (at least) two-fold degeneracy at zero magnetic field. In terms of the electron spin alone,  $\text{Ho}(\text{III})$  is generally described as a non-Kramers ion, while in terms of a  $^{165}\text{Ho}(\text{III})$  particle, which is a fermion, it can be defined as a Kramers system. In a perfect case, this situation will eliminate the mixing between the doublet and can only be broken by intermolecular and/or external magnetic fields.

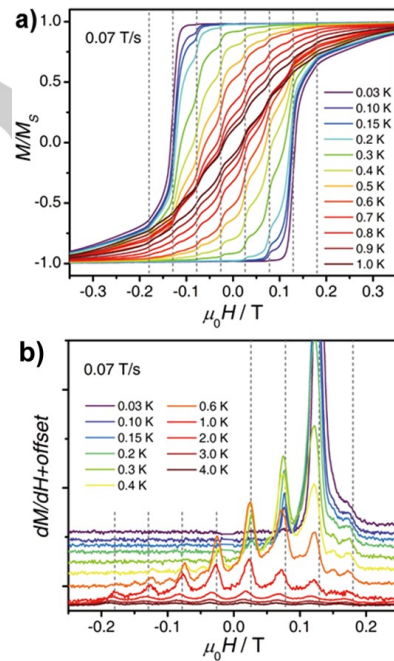


**Figure 5.** a) Normalized magnetic hysteresis loops for single crystal of **1** at a field sweep rate of 0.07 T and the indicated temperatures. b) Derivative of the hysteresis loops ( $dM/dH$  vs.  $H$ , for  $dH/dt > 0$ ). The predicted magnetic field positions of the avoided level crossings of Figure 4 are indicated with gray dashed lines.

To obtain clearer insight into this interesting behavior, magnetization measurements were performed on a single crystal of **1** using a micro-SQUID setup.<sup>12</sup> The field was aligned with the easy axis of magnetization using the transverse field

method.<sup>13</sup> The applied field  $H$  was corrected because the determination of the resonance fields must consider the internal magnetic field of the crystal.<sup>14</sup> Typical hysteresis loops are presented in Figure 5a, showing regular steps that lead to the peaks of the derivative of the loop ( $dM/dH$ ) in Figure 5b and are due to resonant tunneling at the avoided level crossings marked with circles in Figure 4. These hyperfine-structure steps could be observed up to 3 K; see SI.

In conclusion, this work reveals the vast potential of holmium(III) for high-performance SMMs, despite usually being described as a non-Kramers ion. The spin reversal barrier of  $237(4)$  cm<sup>-1</sup> for **1** is an order of magnitude higher than the reported Ho-SIMs to date and only lower than that of {Ho<sub>5</sub>} (278 cm<sup>-1</sup>).<sup>7e</sup> Contrary to some popular belief, the nuclear spin here suppresses (rather than accelerates) the QTM at zero field with the aid of hyperfine interactions. Instead, the avoided level crossings are moved to the in-field area, resulting in field-induced QTM. This behavior might be beneficial for quantum information storage and processing, as the data can be safely kept in the absence of magnetic fields and feasibly manipulated/read out by applying specific external fields. As profound magnetic remanence has recently been observed in individual holmium atoms,<sup>15</sup> we expect these small steps to finally lead to giant leaps in molecular magnetism and quantum devices.

## Acknowledgements

This work was supported by the “973 Project” (2014CB845602), the NSFC (Grant nos. 21620102002, 21371183 and 91422302), the NSF of Guangdong (S2013020013002), and the Humboldt foundation

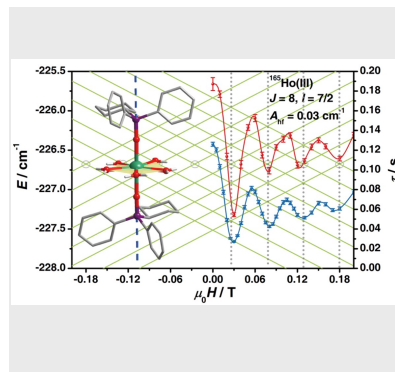
**Keywords:** lanthanide • holmium • magnetic properties • single-molecule magnets • hyperfine interactions

- [1] R. Sessoli, D. Gatteschi, A. Caneschi, M. A. Novak, *Nature* **1993**, *365*, 141–143.
- [2] a) W. Wernsdorfer, *Science* **1999**, *284*, 133–135; b) M. N. Leuenberger, D. Loss, *Nature* **2001**, *410*, 789–793; c) L. Bogani, W. Wernsdorfer, *Nat. Mater.* **2008**, *7*, 179–186; d) M. Mannini, F. Pineider, P. Sainctavit, C. Danieli, E. Otero, C. Sciancalepore, A. M. Talarico, M.-A. Arrio, A. Cornia, D. Gatteschi, R. Sessoli, *Nat. Mater.* **2009**, *8*, 194–197; e) M. Ganzhorn, S. Klyatskaya, M. Ruben, W. Wernsdorfer, *Nat. Nanotechnol.* **2013**, *8*, 165–169; f) S. Thiele, F. Balestro, R. Ballou, S. Klyatskaya, M. Ruben, W. Wernsdorfer, *Science* **2014**, *344*, 1135–1138; g) M. Shiddiq, D. Komijani, Y. Duan, A. Gaita-Ariño, E. Coronado, S. Hill, *Nature* **2016**, *531*, 348–351.
- [3] D. N. Woodruff, R. E. P. Winpenny, R. A. Layfield, *Chem. Rev.* **2013**, *113*, 5110–5148.
- [4] a) S.-D. Jiang, B.-W. Wang, G. Su, Z.-M. Wang, S. Gao, *Angew. Chem. Int. Ed.* **2010**, *49*, 7448–7451; b) J. D. Rinehart, M. Fang, W. J. Evans, J. R. Long, *Nat. Chem.* **2011**, *3*, 538–542; c) R. J. Blagg, L. Ungur, F. Tuna, J. Speak, P. Comar, D. Collison, W. Wernsdorfer, E. J. L. McInnes, L. F. Chibotaru, R. E. P. Winpenny, *Nat. Chem.* **2013**, *5*, 673–678; d) J.-L. Liu, Y.-C. Chen, Y.-Z. Zheng, W.-Q. Lin, L. Ungur, W. Wernsdorfer, L. F. Chibotaru, M.-L. Tong, *Chem. Sci.* **2013**, *4*, 3310–3316; e) Y.-C. Chen, J.-L. Liu, L. Ungur, J. Liu, Q.-W. Li, L.-F. Wang, Z.-P. Ni, L. F. Chibotaru, X.-M. Chen, M.-L. Tong, *J. Am. Chem. Soc.* **2016**, *138*, 2829–2837; f) J. Liu, Y.-C. Chen, J.-L. Liu, V. Vieru, L. Ungur, J.-H. Jia, L. F. Chibotaru, Y. Lan, W. Wernsdorfer, S. Gao, X.-M. Chen, M.-L. Tong, *J. Am. Chem. Soc.* **2016**, *138*, 5441–5450; g) S. K. Gupta, T. Rajeshkumar, G. Rajaraman, R. Murugavel, *Chem. Sci.* **2016**, *7*, 5181–5191; h) Y.-S. Ding, N. F. Chilton, R. E. P. Winpenny, Y.-Z. Zheng, *Angew. Chem. Int. Ed.* **2016**, *55*, 16071–16074.
- [5] a) S.-D. Jiang, B.-W. Wang, H.-L. Sun, Z.-M. Wang, S. Gao, *J. Am. Chem. Soc.* **2011**, *133*, 4730–4733; b) K. R. Meihaus, J. R. Long, *J. Am. Chem. Soc.* **2013**, *135*, 17952–17957; c) L. Ungur, J. J. Le Roy, I. Korobkov, M. Murugesu, L. F. Chibotaru, *Angew. Chem. Int. Ed.* **2014**, *53*, 4413–4417; d) J. J. Le Roy, L. Ungur, I. Korobkov, L. F. Chibotaru, M. Murugesu, *J. Am. Chem. Soc.* **2014**, *136*, 8003–8010.
- [6] a) N. Ishikawa, M. Sugita, T. Ishikawa, S.-y. Koshihara, Y. Kaizu, *J. Am. Chem. Soc.* **2003**, *125*, 8694–8695; b) N. Ishikawa, S. Otsuka, Y. Kaizu, *Angew. Chem. Int. Ed.* **2005**, *44*, 731–733; c) N. Ishikawa, M. Sugita, W. Wernsdorfer, *Angew. Chem. Int. Ed.* **2005**, *44*, 2931–2935; d) F. Branzoli, P. Caretta, M. Filibian, G. Zoppellaro, M. J. Graf, J. R. Galan-Mascaros, O. Fuhr, S. Brink, M. Ruben, *J. Am. Chem. Soc.* **2009**, *131*, 4387–4396; e) S. Osa, T. Kido, N. Matsumoto, N. Re, A. Pochaba, J. Mrozník, *J. Am. Chem. Soc.* **2003**, *126*, 420–421; f) J. D. Rinehart, M. Fang, W. J. Evans, J. R. Long, *J. Am. Chem. Soc.* **2011**, *133*, 14236–14239; g) K. Katoh, B. K. Breedlove, M. Yamashita, *Chem. Sci.* **2016**, *7*, 4329–4340.
- [7] a) N. Ishikawa, M. Sugita, W. Wernsdorfer, *J. Am. Chem. Soc.* **2005**, *127*, 3650–3651; b) S. Cardona-Serra, J. M. Clemente-Juan, E. Coronado, A. Gaita-Ariño, A. Camón, M. Evangelisti, F. Luis, M. J. Martínez-Pérez, J. Sesé, *J. Am. Chem. Soc.* **2012**, *134*, 14982–14990; c) S. Ghosh, S. Datta, L. Friend, S. Cardona-Serra, A. Gaita-Ariño, E. Coronado, S. Hill, *Dalton Trans.* **2012**, *41*, 13697–13704; d) J. Dreiser, R. Westerström, Y. Zhang, A. A. Popov, L. Dunsch, K. Krämer, S.-X. Liu, S. Decurtins, T. Greber, *Chem. Eur. J.* **2014**, *20*, 13536–13540; e) R. J. Blagg, F. Tuna, E. J. L. McInnes, R. E. P. Winpenny, *Chem. Commun.* **2011**, *47*, 10587–10589.
- [8] F. Pointillart, K. Bernot, S. Golhen, B. Le Guennic, T. Guizouarn, L. Ouahab, O. Cador, *Angew. Chem. Int. Ed.* **2015**, *54*, 1504–1507.
- [9] a) F. Aquilante, J. Autschbach, R. K. Carlson, L. F. Chibotaru, M. G. Delcey, L. De Vico, I. Fdez. Galván, N. Ferré, L. M. Frutos, L. Gagliardi, M. Garavelli, A. Giussani, C. E. Hoyer, G. Li Manni, H. Lischka, D. Ma, P. Å. Malmqvist, T. Müller, A. Nenov, M. Olivucci, T. B. Pedersen, D. Peng, F. Plasser, B. Pritchard, M. Reiher, I. Rivalta, I. Schapiro, J. Segarra-Martí, M. Stenrup, D. G. Truhlar, L. Ungur, A. Valentini, S. Vancoillie, V. Veryazov, V. P. Vysotskiy, O. Weingart, F. Zapata, R. Lindh, *J. Comput. Chem.* **2016**, *37*, 506–541; b) L. Ungur, L. F. Chibotaru in *Lanthanides and Actinides in Molecular Magnetism* (Eds.: R. A. Layfield, M. Murugesu), Wiley-VCH, Weinheim, **2015**.
- [10] L. Ungur, L. F. Chibotaru, *Inorg. Chem.* **2016**, *55*, 10043–10056.
- [11] a) R. Giraud, W. Wernsdorfer, A. M. Tkachuk, D. Mailly, B. Barbara, *Phys. Rev. Lett.* **2001**, *87*, 057203; b) W. Salomon, Y. Lan, E. Rivière, S. Yang, C. Roch-Marchal, A. Dolbecq, C. Simonnet-Jégat, N. Steunou, N. Leclerc-Laronze, L. Ruhlmann, T. Mallah, W. Wernsdorfer, P. Mialane, *Chem. Eur. J.* **2016**, *22*, 6564–6574.
- [12] a) W. Wernsdorfer in *Advances in Chemical Physics*, Vol. 118 (Eds.: I. Prigogine, S. A. Rice), John Wiley & Sons, Inc., Hoboken, **2001**, pp. 99–190; b) W. Wernsdorfer, *Supercond. Sci. Technol.* **2009**, *22*, 064013.
- [13] W. Wernsdorfer, N. E. Chakov, G. Christou, *Phys. Rev. B* **2004**, *70*, 132413.
- [14] W. Wernsdorfer, M. Murugesu, G. Christou, *Phys. Rev. Lett.* **2006**, *96*, 057208.
- [15] F. Donati, S. Rusponi, S. Stepanow, C. Wäckerlin, A. Singha, L. Persichetti, R. Baltic, K. Diller, F. Patthey, E. Fernandes, J. Dreiser, Ž. Šljivančanin, K. Kummer, C. Nistor, P. Gambardella, H. Brune, *Science* **2016**, *352*, 318–321.

## Entry for the Table of Contents

## COMMUNICATION

An extremely rare non-Kramers holmium(III) single-ion magnet (SIM) is reported with a high energy barrier of  $237(4)$  cm $^{-1}$ . The suppression of quantum tunneling of magnetization (QTM) at zero field and the hyperfine structures can be observed from AC magnetic susceptibility, which is attributed to the combination of the favorable crystal-field environment and the hyperfine interactions arising from  $^{165}\text{Ho}$  ( $I = 7/2$ ) with a natural abundance of 100 %.



Yan-Cong Chen,<sup>[a]</sup> Jun-Liang Liu, \*<sup>[a]</sup>  
Wolfgang Wernsdorfer,<sup>[b][c][d]</sup> Dan Liu,<sup>[e]</sup>  
Liviu F. Chibotaru,<sup>[e]</sup> Xiao-Ming Chen,<sup>[a]</sup>  
and Ming-Liang Tong,<sup>\*[a]</sup>

Page No. – Page No.

Hyperfine Interaction-Driven  
Suppression of Quantum Tunneling  
at Zero Field in a Ho(III) Single-Ion  
Magnet